Crystal symmetry of stripe-ordered $La_{1.88}Sr_{0.12}CuO_4$

R. Frison,[1] J. Küspert,[1] Qisi Wang,[1] O. Ivashko,[2] M. v. Zimmermann,[2] M. Meven,[3,4] D. Bucher,[1] J. Larsen,[5,6] Ch. Niedermayer,[7] M. Janoschek,[1,8] T. Kurosawa,[9] N. Momono,[9,10] M. Oda,[9] N. B. Christensen,[5,*] and J. Chang[1]

[1]*Physik-Institut, Universität Zürich, Winterthurerstrasse 190, CH-8057 Zürich, Switzerland*
[2]*Deutsches Elektronen-Synchrotron DESY, Notkestraße 85, 22607 Hamburg, Germany*
[3]*RWTH Aachen University, Institut für Kristallographie, 52056 Aachen, Germany*
[4]*Jülich Centre for Neutron Science (JCNS) at Heinz Maier-Leibnitz Zentrum (MLZ), 85747 Garching, Germany*
[5]*Department of Physics, Technical University of Denmark, DK-2800 Kongens Lyngby, Denmark*
[6]*Danish Fundamental Metrology A/S, Kogle Allé 5, 2970 Hørsholm, Denmark*
[7]*Laboratory for Neutron Scattering and Imaging, Paul Scherrer Institut, CH-5232 Villigen PSI, Switzerland*
[8]*Laboratory for Neutron and Muon Instrumentation, Paul Scherrer Institut, CH-5232 Villigen PSI, Switzerland*
[9]*Department of Physics, Hokkaido University - Sapporo 060-0810, Japan*
[10]*Department of Sciences and Informatics, Muroran Institute of Technology, Muroran 050-8585, Japan*

(Received 13 January 2022; revised 21 April 2022; accepted 2 May 2022; published 27 June 2022; corrected 18 July 2022)

We present a combined x-ray and neutron diffraction study of the stripe-ordered superconductor $La_{1.88}Sr_{0.12}CuO_4$. The average crystal structure is consistent with the orthorhombic *Bmab* space group as commonly reported in the literature. This structure, however, is not symmetry compatible with a second-order phase transition into the stripe order phase, and as we report here, numerous Bragg peaks forbidden in the *Bmab* space group are observed. We have studied and analyzed these *Bmab*-forbidden Bragg reflections. Fitting of the diffraction intensities yields monoclinic lattice distortions that are symmetry consistent with charge stripe order.

DOI: 10.1103/PhysRevB.105.224113

I. INTRODUCTION

The average crystal structure across the cuprate high-temperature superconducting phase diagrams was determined early on by means of neutron and x-ray diffraction (XRD) [1–6]. Although superconductivity in the cuprates is unlikely driven by phonons, the atomic lattice coordination still has relevance. For example, charge-density waves (CDW) competing with superconductivity are associated with lattice strain waves distorting the lattice away from the average structure. In underdoped $YBa_2Cu_3O_{6+x}$ (YBCO), for example, the average structure is described by the space group *Pmmm* whereas the charge ordering strain waves break the mirror symmetry of the CuO_2 bilayers generating a supercell with the same space group *Pmmm* symmetry [7].

For La-based cuprates, however, the strain wave-induced subgroup crystal structure remains unsolved. The discovery of thermal Hall effect in $La_{2-x}Sr_xCuO_4$ (LSCO) [8–10] has been interpreted in terms of chiral phonon excitations that would require specific crystal structures. While it seems established that the average structure of LSCO can be well described by the orthorhombic space group *Bmab* (space group 64) [6,11], increasing evidence suggests the presence of additional subtle structural distortions both in doped and undoped LSCO. Forbidden Bragg reflections (systematic extinctions) [12] in the space group 64 have already been reported and in some cases interpreted as a consequence of a different —local— crystal structure at the twin boundaries [13–16]. Neutron diffraction experiments performed at room temperature on detwinned La_2CuO_4 (LCO) and very underdoped LSCO single crystals [17] revealed the observation of weak symmetry forbidden Bragg reflections. The existence of such peaks was interpreted as a deviation from the orthorhombic symmetry *Bmab* to a monoclinic $B2/m$, thus preserving lattice centering. Such results were later confirmed in similar experiments on lightly doped and twinned $La_{1.95}Sr_{0.05}CuO_4$ reporting a weak but persistent monoclinic distortion reaching its maximum below 50 K and gradually decreasing, without vanishing through a first-order phase transition, up to 250 K [18]. More recently, a reinvestigation of the LCO crystal symmetry [19] showed, along with the $B2/m$ peaks, evidence of the loss of lattice centering due to the observation of Bragg peaks with odd-odd indices in the $(hk0)$ plane and weak signatures of the $B2/m$ monoclinic peaks up to 500 K. It has thus been proposed [19] that there is a possible direct transition from the high-temperature tetragonal (HTT) phase to the monoclinic structure. In parallel, CDW order in LSCO has been reported with wave vector $\boldsymbol{q} = (\simeq \pm 1/4, 0, 1/2)$ [15,20]. The emergence of CDW order can be interpreted as the consequence of a displacive continuous phase transition where the space group symmetries, before and after the transition, are connected by a group–subgroup relation. Group theory [21–23] indicates which of the possible modulated displacement patterns are consistent with the observed CDW ordering wave vectors. Symmetry analysis indicates that the stripe order observed in the LSCO system is not consistent with space group 64 as in this space group the

*nbch@fysik.dtu.dk.

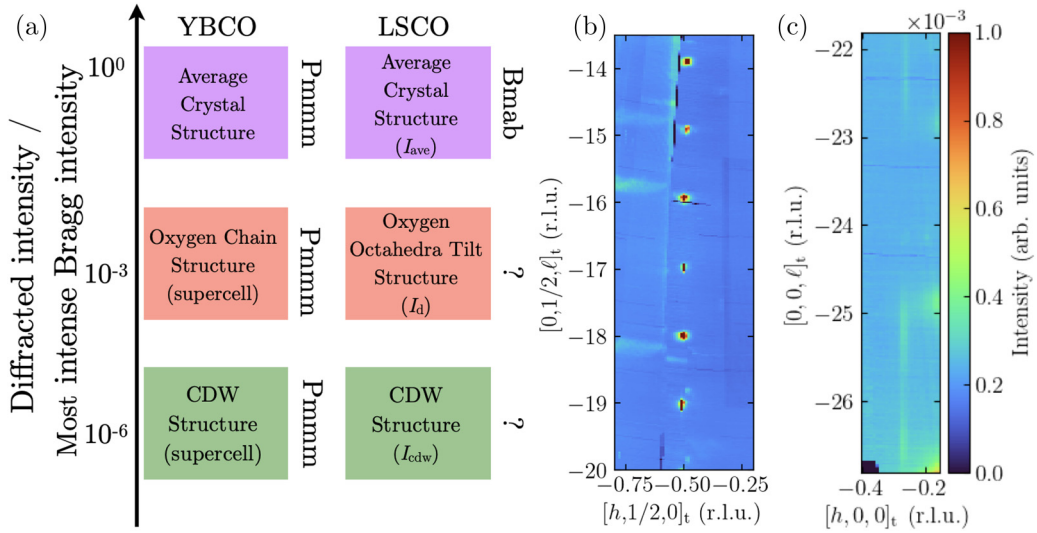

FIG. 1. (a) Hierarchy of Bragg reflection intensity and crystal structure in YBCO and LSCO. Scattering intensity normalized to the most intense Bragg reflection is shown schematically. Intense fundamental lattice Bragg reflection are used for crystal structure determination. In both LSCO and YBCO, the CDW reflections are $10^{-6} - 10^{-7}$ times weaker than the fundamental Bragg reflections. Oxygen chain order in YBCO and monoclinic distortion in LSCO manifest by moderately weak reflections in the ratio $10^{-2} - 10^{-3}$ to that of fundamental Bragg reflections. For YBCO the crystal structure (including oxygen chain order) is determined to be *Pmmm* and the CDW order generates a supercell with *Pmmm* symmetry. The crystal structure of LSCO is not determined with the same precision. The average crystal structure defined by the strongest fundamental Bragg reflection is *Bmab* (orthorhombic space group 64). However, the monoclinic and CDW reflections are inconsistent with this average structure. The crystal symmetry of LSCO is therefore unsolved. (b) Portion of the reconstructed $(h, 1/2, \ell)_t$ plane showing some of *Bmab*-forbidden peaks. Gaussian fits of the *Bmab*-forbidden peaks along the h, k, and ℓ principal axes indicate that the correlation length ξ along a and b directions is at least 50 unit cells, while along c $\xi \gtrapprox 10c$. Peaks of the kind $(o, 0, e)$ belong to the second twin component. (c) Section of the reconstructed $(h, 0, \ell)_t$ of reciprocal space along with CDW signal.

$[1, 0, 0]_t$ and $[0, 1, 0]_t$ directions and all the CuO_6 octahedra are equivalent [24]. In $La_{1.85}Ba_{0.15}CuO_4$, for example, a direct tetragonal to monoclinic transition rather than a tetragonal to orthorhombic transition has been proposed [25,26]. Experimental evidence [16,17,19] shows that the LSCO system displays a hierarchy of lattice reflections as shown schematically in Fig. 1(a). The strongest reflections define the average structure (I_{ave}). Weak *Bmab*-forbidden peaks with intensity $I_d \approx \delta I_{ave}$ correspond to subtle lattice distortions with δ ranging from 10^{-3} to 10^{-2} Figs. 2(a)–2(f). Finally, there are charge order-induced strain wave reflections for which $I_{cdw} \approx 10^{-6}$-$10^{-7} I_{ave}$, see Figs. 1(b)–1(c). It is, therefore, important to solve the subgroup crystal structure problem accounting for the observed, coexisting, weak structural distortions.

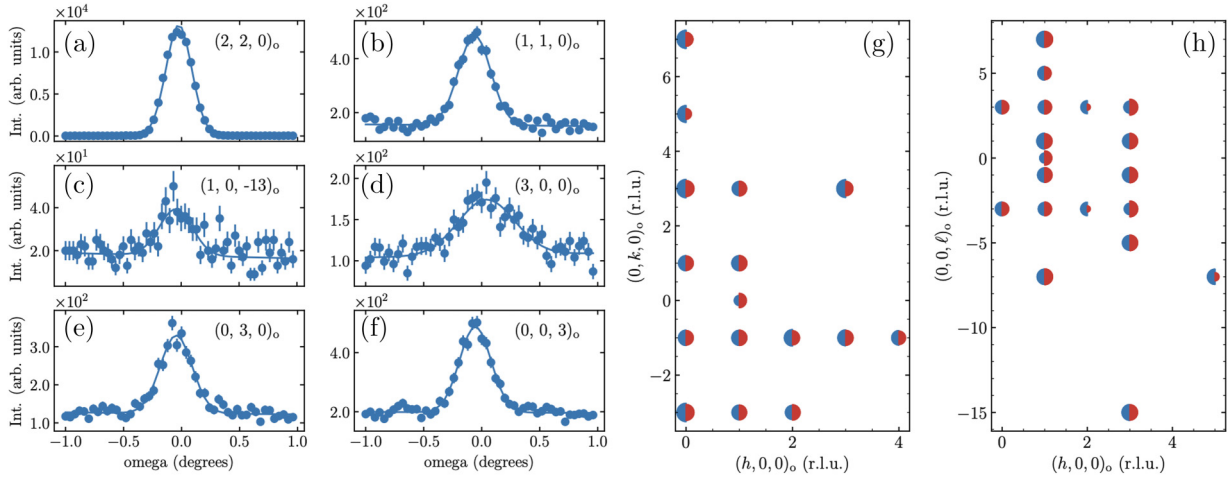

FIG. 2. Allowed and forbidden Bragg peaks measured on $La_{1.88}Sr_{0.12}CuO_4$ by neutron diffraction. (a)–(f) Bragg peaks indexed using orthorhombic *Bmab* notation. (a) Allowed Bragg reflection, $(2, 2, 0)_o$; (b)–(f) Forbidden Bragg peaks of the kind $(o, o, 0)_o$, $(o, 0, o)_o$, $(o, 0, 0)_o$, $(0, o, 0)_o$, and $(0, 0, o)_o$ with o being an odd integer (see also the text). The line through the data points is a Gaussian fit to guide the eye. (g), (h) Observed (blue half circle) and fitted (red half circle) neutron diffraction intensities of *Bmab*-forbidden peaks using the $P2/m$ model for the $(h, k, 0)$ and $(h, 0, \ell)$ planes. The radius of the semicircles is proportional to the intensity of the corresponding Bragg peaks.

Here we analyze the deviations from the average structure in a $La_{1.88}Sr_{0.12}CuO_4$ crystal. We have carried out neutron and x-ray single-crystal diffraction (XRD) experiments. In the former, the crystal was not detwinned, whereas in the latter, uniaxial pressure was applied along a copper-oxygen bond direction (a_t) to minimize twinning effects. We performed a systematic study of the symmetry forbidden Bragg peaks of the average structure. Our results are analyzed and discussed by identifying subgroups of the established average orthorhombic (*Bmab*) structure consistent consistent with the observed forbidden Bragg peaks, and via crystal structure refinement of the model candidates to identify the space group providing the best fit of the observed *Bmab*-forbidden Bragg peaks.

II. METHODS

We performed neutron diffraction experiment using a 5 mm $\times \oslash$ 5 mm $La_{1.88}Sr_{0.12}CuO_4$ single crystal ($T_c = 27$ K) grown by the traveling solvent floating zone method [27,28]. Neutron diffraction data were collected at the HEiDi Single-crystal diffractometer at neutron source FRM-II of the Heinz Maier-Leibnitz Zentrum (MLZ) in Garching near Munich using an Erbium filter with $\lambda = 0.7094$ Å and $q_{max} = 2\sin(\theta)/\lambda = 0.97$ Å^{-1}. For the x-ray experiments on the same crystal batch, uniaxial pressure was applied *ex situ*, as described in Ref. [29], along a Cu-O bond direction ($\boldsymbol{a}_t$ or $\boldsymbol{b}_t$) to minimize orthorhombic twinning effects. XRD data collection was performed at the P21.1 beamline at PETRA-III (Hamburg) synchrotron using $\lambda = 0.122$ Å in combination with a PerkinElmer or a Dectris Pilatus 100K CdTe detector. Data indexing and integration was performed using XDS [30]. Crystal structure refinement was done using Shelxl [31] and structure factor calculation of the distorted superstructure was performed using the FULLPROF SUITE [32]. Throughout the text, reciprocal space is indexed according to the HTT structure as $(h, k, \ell)_t$, or according to the average low temperature orthorhombic structure as $(h, k, \ell)_o$. The two indexing notations are connected by $(h, k, \ell)_o = R_{\frac{\pi}{4}}(h, k, \ell)_t$ where $R_{\frac{\pi}{4}}$ is a matrix rotation around the (0,0,1) axis. The choice of adopting the two indexing schemes reflects the fact that, throughout the existing literature, charge stripe order in LSCO is indicated in tetragonal notation, while distortions away from space group 64 are best described in orthorhombic notation.

III. RESULTS

CDW stripe order manifests by reflections at $\boldsymbol{Q} = \boldsymbol{\tau} + (\delta, 0, 1/2)_t$ with $\delta \simeq 1/4$ and $\boldsymbol{\tau}$ being a fundamental Bragg position. Figures 1(b) and 1(c) display sections of the reconstructed reciprocal space probed by XRD around $(1/4, 0, \ell)_t = (1/4, 1/4, \ell)_o$ and $(-1/2, 1/2, \ell)_t = (-1, 0, \ell)_o$ across multiple Brillouin zones along the reciprocal c axis. The out-of-plane charge order correlation length is small and hence the intensity, peaking at half integer values of ℓ, extends across the entire Brillouin zone. The three-dimensional peaks at $(-0.5, 0.5, o)_t$, with o being an odd integer, correspond to $(-1, 0, o)_o$ in *Bmab* orthorhombic notation. In addition to the $(o, 0, o)_o$ reflections, weak Bragg peaks of the kind $(e, o, 0)_o$ with e being an even integer are observed; see Figs. 3(a)–3(b). These reflection conditions cannot be explained even taking into account the presence of orthorhombic twin domains [11,33] and are therefore inconsistent with the space group *Bmab*. The observed reflection conditions are consistent with the monoclinic space group $B2/m(11)$, in agreement with previous results [17,18].

TABLE I. Space groups notations and their reflection conditions. Conditions are abbreviated assuming the expression is an even number [12].

Space group		Reflection conditions							
Symbol	No.	$hk\ell$	$hk0$	$h0\ell$	$0k\ell$	$hh\ell$	$h00$	$0k0$	00ℓ
$I4/mmmm$	139	$h+k+\ell$	$h+k$		$k+\ell$	ℓ		k	ℓ
Bmab	64	$h+\ell$	h, k	h, ℓ	ℓ		h	k	ℓ
$B2/m(11)$	12	$h+\ell$	$h+\ell$	$h+\ell$	ℓ		h		
$P2/m(11)$	10								
$Bm(11)$	8	$h+\ell$	$h+\ell$	$h+\ell$	ℓ		h		
$P2_1(11)$	4						h		

To exclude uniaxial pressure as the cause for symmetry reduction, we carried out a neutron diffraction experiment on a $La_{1.88}Sr_{0.12}CuO_4$ crystal without uniaxial pressure applied. This data set also displays weak reflections, with odd indices along the $h00$, $0k0$, and 00ℓ axes and of the kind $(e, e, o)_o$, $(o, o, 0)_o$, $(e, o, 0)_o$, and $(o, 0, o)_o$ which are inconsistent with the space group *Bmab* [Figs. 2(b)–2(f)] and cannot be explained by the twin law [11]. In this case, the observed reflection conditions indicate the space group $P2_1$ (4), in agreement with recent observations [19]. We note, however, that in this case the $(h, 0, 0)$ condition imposed by the space group $P2_1$, is masked by the presence of orthorhombic twins. Thus also the space group $P2/m$ is a plausible structure. Reflection conditions for the various space groups are reported in Table I. Before attempting a finer crystal structure refinement, we notice that the x-ray and neutron diffraction experiments provide some overlap of "forbidden" Bragg peaks, yet the two data sets are not identical and hence are analyzed separately (Table II).

IV. ANALYSIS

For the neutron data set, we performed refinements using the space groups $P2_1$ and $P2/m$ obtaining R = 0.0974 and R = 0.0776, respectively; see Table III. For the x-ray data set we tested the monoclinic space groups *Bm* and $B2/m$,

TABLE II. Modulation amplitudes (in Å) for each $La_{1.88}Sr_{0.12}CuO_4$ HTT site; '—-" marks amplitudes fixed to zero by symmetry; "0" marks amplitudes fixed manually to zero.

	$P2/m$		$B2/m$
Atom	X_1^+	X_4^+	X_1^+
La	0.0055(3)	0	−0.0010(9)
Sr	0.0055(3)	0	−0.0010(9)
Cu	—	—	—
O1	−0.057(1)	−0.2(1)	−0.12(1)
O2	0.128(2)	0.21(2)	0.10(1)

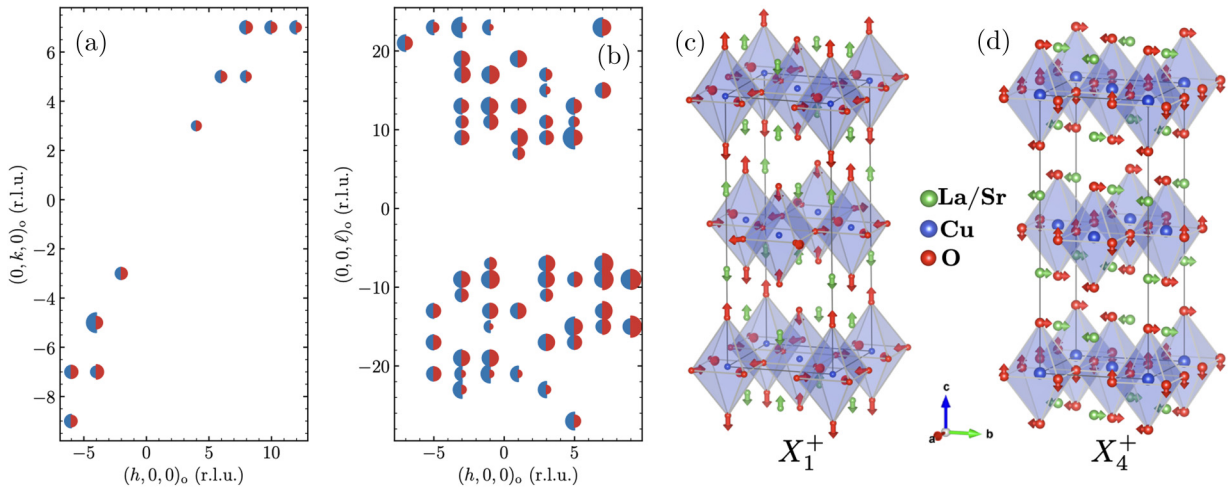

FIG. 3. (a), (b) Observed (blue half circle) and fitted (red half circle) XRD intensities of *Bmab*-forbidden peaks using the $B2/m$ model for the $(h, k, 0)$ and $(h, 0, \ell)$ planes. The radius of the semicircles is proportional to the intensity of the corresponding Bragg peaks. (c), (d) Representation of the atomic displacement motifs according to distortion modes (c) X_1^+ and (d) X_4^+ for an undistorted unit cell; the magnitude of the displacements has been exaggerated to make them visible.

obtaining, respectively, R = 0.081 and R = 0.077; see Table IV. In all these cases the intensity of the *Bmab*-forbidden Bragg peaks is underestimated. Further, the Wilson statistic $\langle |E^2 - 1| \rangle$ is 1.3 and 1.5 for the neutron and x-ray case, indicating the presence of a centrosymmetric structure. Single-crystal structure refinements favor the *Bmab* space group for both our x-ray and neutron diffraction experiments. Therefore to provide a better fit to the forbidden peaks, we opted for partitioning the total intensity as $I_{\text{tot}} \simeq I_{\text{ave}} + I_{\text{d}}$ where subscripts stand for total, average, and distortion, respectively. Our working hypothesis is that the average structure is equivalent to the *Bmab* space group and the weaker distortions represent small, static, correlated—symmetry breaking—atomic displacements away from the average structure [34]. The structural distortion component is further described in terms of mode superposition. Each mode is a collective correlated atomic displacements pattern fulfilling specific symmetry properties given by the irreducible representations (irreps) of the undistorted parent high-symmetry space group [21,35,36,37].

To discuss the structural distortions in $La_{1.88}Sr_{0.12}CuO_4$, we start from the parent high-symmetry tetragonal $I4/mmm$ structure. Orthorhombic structures manifest, in the first Brillouin zone, at $X = (1/2, 1/2, 0)_t$ [38–40]. Group theory indicates that there are seven displacement patterns (irreps) consistent with this observed wave vector [41]: X_1^+, X_2^+, X_3^+, X_4^+, X_2^-, X_3^-, X_4^-. The *Bmab* structure, for example, corresponds to a CuO_6 octahedral tilt in the $[1, 1, 0]_t = [0, 1, 0]_o$ direction. This distortion pattern is described by the X_3^+ irrep. In the same fashion, the monoclinic space groups, $P2/m$ and $B2/m$, are induced by the couplings $X_1^+ \oplus X_3^+ \oplus X_4^+$ and $X_1^+ \oplus X_3^+$, respectively. The X_1^+ mode consists in a correlated displacement of the octahedral in-plane oxygens along the tetragonal in-plane axes and along the out-of-plane tetragonal axis of the octahedral apical oxygen atoms. The X_4^+ mode, instead, involves a tilt of the CuO_6 octahedra around an in-plane axis, with octahedra in the first and second layer tilting out of phase. The X_1^+ and X_4^+ distortion patterns are illustrated in Figs. 3(c) and 3(d). We fitted the intensities of the *Bmab*-forbidden peaks optimizing the mode amplitudes of the X_1^+ mode (x-ray) and X_1^+, X_4^+ modes (neutron), as these are the distinctive modes of the distorted structure. As shown in Fig. 2 and Fig. 3, reasonable agreement is obtained for both the neutron and the XRD experiments. The agreement factor $(\sum_i |I_i^{\text{obs}} - I_i^{\text{calc}}|^2/\sigma_i)/(\sum_i (I_i^{\text{obs}})^2/\sigma_i)$ for the two refinements is 7.4 and 18.0%, respectively. The mode amplitudes for each atomic site are given in Table II.

We now extend our symmetry analysis to include charge order. Stripe order in LSCO is characterized by a uniaxial ordering vector $\boldsymbol{Q} \sim (1/4, 0, 1/2)_t$ [15,20,42]. This is contrast with YBCO, where a bidirectional CDW structure is reported [43–45]. The monodirectional stripe ordering vector of LSCO induces a further symmetry reduction which can be accounted for by a unit cell multiplication consistent with the ordering vector $\boldsymbol{Q} \sim (1/4, 0, 1/2)_t$. As shown above, the existence of *Bmab*-forbidden Bragg peaks indicate monoclinic distortions which are described by specific irreps (X_1^+ and X_4^+). Group theory indicates [41] that the CDW wave vector corresponds to the irreps B_1, B_2. By coupling B with the other irreps (determined on the basis of the average and monoclinic distortion), stripe order remains consistent with both $B2/m$ and $P2/m$ space groups.

V. DISCUSSION

Different monoclinic structures are observed under ambient and uniaxial pressure application suggesting that uniaxial pressure influences the correlation of the weak lattice distortions. On the modeling side we find relatively high fit agreement factors, particularly for the x-ray data set. We note that LSCO is characterized by intrinsic chemical disorder. In fact, while the average structure refinement confirms the *Bmab* (LTO) structure as the best-fitting model (see Table V), we found residual electron density peaks around the La/Sr position, which is not resolved refining the La(Sr) site occupation factor. It is thus expected that also the weak structural distortion, and its corresponding intensity distribution, can be

TABLE III. Positional and thermal parameters of $La_{1.88}Sr_{0.12}CuO_4$ as obtained from the structure refinement of the neutron diffraction data sets using the $P2_1$ (top) and $P2/m$ (bottom).

$La_{1.88}Sr_{0.12}CuO_4$ at 2 K, neutron diffraction $\lambda = 0.794$ Å: $a = 5.34(4)$ Å $b = 5.37(7)$ Å $c = 13.22(0)$ Å $\alpha = \beta = \gamma = 90$ deg; $P2_1$ symmetry, extinction coefficient = 0.037(6), twin fraction = 0.204(4); R = 9.74%, wR2 = 25.17%, GooF = 1.535.

Atom	Site	x	y	z	U_{eq}	Occ.
La	2*a*	0.7547(6)	−0.0004(5)	0.3576(2)	0.00037	0.875
Sr	2*a*	0.7547(6)	−0.0004(5)	0.3576(2)	0.00037	0.125
La	2*a*	0.2460(6)	−0.0104(5)	0.8637(2)	0.00006	0.875
Sr	2*a*	0.2460(6)	−0.0104(5)	0.8637(2)	0.00006	0.125
La	2*a*	0.7464(7)	0.0112(5)	0.6424(2)	0.00054	0.875
Sr	2*a*	0.7464(7)	0.0112(5)	0.6424(2)	0.00054	0.125
La	2*a*	0.2535(6)	0.0017(5)	0.1357(2)	0.00053	0.875
Sr	2*a*	0.2535(6)	0.0017(5)	0.1357(2)	0.00053	0.125
Cu	2*a*	0.7498(6)	−0.0039(9)	0.0001(2)	0.001	1.0
Cu	2*a*	0.251(1)	0.007(2)	0.5003(5)	0.0168	1.0
O	2*a*	0.002(1)	0.751(4)	0.0055(6)	0.010(1)	1.0
O	2*a*	0.4988(8)	0.7504(8)	0.5033(4)	0.0014(6)	1.0
O	2*a*	0.502(1)	0.251(1)	−0.0096(6)	0.0086(9)	1.0
O	2*a*	-0.0002(8)	0.2505(9)	0.4943(5)	0.0018(7)	1.0
O	2*a*	0.755(1)	0.031(1)	0.1831(5)	0.0097(9)	1.0
O	2*a*	0.2492(9)	0.0244(9)	0.6819(4)	0.0059(6)	1.0
O	2*a*	0.754(1)	−0.031(1)	0.8179(4)	0.0072(7)	1.0
O	2*a*	0.249(1)	−0.026(1)	0.3171(4)	0.0078(8)	1.0

$La_{1.88}Sr_{0.12}CuO_4$ at 2 K, neutron diffraction $\lambda = 0.794$ Å: $a = 5.34(4)$ Å $b = 5.37(7)$ Å $c = 13.22(0)$ Å $\alpha = \beta = \gamma = 90$ deg; $P2/m$ symmetry, extinction coefficient = 0.027(4), twin fraction = 0.204(4); R = 7.76%, wR2 = 20.95%, GooF = 1.295.

La	2*m*	0	0.0059(7)	0.3621(3)	0.0004(–)	0.4685
Sr	2*m*	0	0.0059(7)	0.3621(3)	0.0004(–)	0.03125
La	2*n*	1/2	0.0060(8)	0.8592(3)	0.0021(3)	0.4685
Sr	2*n*	1/2	0.0060(8)	0.8592(3)	0.0021(3)	0.03125
La	2*m*	0	0.5064(7)	0.1410(3)	0.0024(4)	0.4685
Sr	2*m*	0	0.5064(7)	0.1410(3)	0.0024(4)	0.0312
La	2*n*	1/2	0.5061(6)	0.6376(2)	0.0011(4)	0.4685
Cu	1*a*	0	0	0	0.001(–)	0.25250
Cu	1*e*	1/2	0	1/2	0.001(–)	0.25250
Cu	1*f*	1/2	1/2	0	0.0060(3)	0.25250
Cu	1*g*	0	1/2	1/2	0.0060(3)	0.25250
O	4*o*	0.2495(4)	0.7498(3)	0.49527(13)	0.00030(–)	1.0
O	4*o*	0.7509(6)	0.7500(5)	-0.0074(2)	0.0089(3)	1.0
O	2*m*	0	−0.0307(9)	0.1826(4)	0.0082(8)	0.5
O	2*n*	1/2	−0.0269(8)	0.6826(4)	0.0052(7)	0.5
O	2*m*	0	0.4750(9)	0.3179(4)	0.0058(7)	0.5
O	2*a*	1/2	0.4691(9)	0.8173(4)	0.0064(7)	0.5

affected by the presence of some occupational disorder. As a consequence, also the fitness of our distortion model, which is only sensitive to the periodic features of the structure but responsible for the forbidden reflections, would be affected. The fitting model reproduces most of the modulations of the observed intensities; see Figs. 3(a) and 3(b). As represented in Figs. 3(c) and 3(d, the model describes correlated in-plane and out-of-plane displacements of the octahedral oxygen atoms such that in corner-sharing octahedra the displacement has an opposite sign.

Monoclinic distortions have also been reported for the parent $La_{2-x}Sr_xCuO_4$ and lightly doped compound [17–19], where a thermal Hall effect has also been reported [8–10] and interpreted in terms of chiral phonon excitations that would require specific crystal structures. In this context, the connection between the observed monoclinic distortions and thermal Hall effect could be tested by uniaxial pressure that seems to tune the former.

The present situation here described for LSCO shows some analogy and some difference with the case of YBCO. In YBCO different reciprocal space superstructures with periodicity $1/m$ ($m = 2, 3, 4, 5, 8$) along the $\boldsymbol{a}^*$ axis have been reported [44,46]. Each of these corresponds to a specific ordering pattern of the chain oxygens [46] thus with periodicity

TABLE IV. Positional and thermal parameters of $La_{1.88}Sr_{0.12}CuO_4$ as obtained from the structure refinement of the XRD data sets using the *Bm* (top) and $B2/m$ (bottom).

$La_{1.88}Sr_{0.12}CuO_4$ at 30 K, XRD $\lambda = 0.122$ Å: $a = 5.31(9)$ Å $b = 5.33(9)$ Å $c = 13.17(9)$ Å $\alpha = \beta = \gamma = 90$ deg; *Bm* symmetry, extinction coefficient = 0.48(5), twin fraction = 0.121(2); R = 8.07%, wR2 = 16.54%, GooF = 1.54.

Atom	site	x	y	z	U_{eq}	Occ.
La	2*a*	0	0.00457(5)	0.36098(2)	0.00112(7)	0.4375
Sr	2*a*	0	0.00457(5)	0.36098(2)	0.00112(7)	0.0625
La	2*a*	0	−0.00425(5)	0.63904(2)	0.00105(7)	0.4375
Sr	2*a*	0	−0.00425(5)	0.63904(2)	0.00105(7)	0.0625
La	2*a*	0	0.49517(5)	0.86096(2)	0.00111(6)	0.4375
Sr	2*a*	0	0.49517(5)	0.86096(2)	0.00111(6)	0.0625
La	2*a*	0	0.50464(5)	0.13903(2)	0.00104(7)	0.4375
Sr	2*a*	0	0.50464(5)	0.13903(2)	0.00104(7)	0.0625
Cu	2*a*	0	−0.0035(4)	−0.00030(17)	0.00151(8)	0.5
Cu	2*a*	0	0.4975(5)	0.49968(17)	0.00159(8)	0.5
O	4*b* 0.7502(5)	0.2514(10)	0.0049(2)	0.0047(3)	1.0	
O	4*b*	0.2500(5)	0.7517(10)	0.4958(2)	0.0054(3)	1.0
O	2*a*	0	−0.0217(11)	0.1813(2)	0.0095(5)	0.5
O	2*a*	0	0.0291(13)	0.8171(3)	0.0063(5)	0.5
O	2*a*	0	0.5298(7)	0.68289(16)	0.0021(2)	0.5
O	2*a*	0	0.4920(15)	0.3193(4)	0.0172(10)	0.5

$La_{1.88}Sr_{0.12}CuO_4$ at 30 K, XRD $\lambda = 0.122$ Å: $a = 5.31(9)$ Å $b = 5.33(9)$ Å $c = 13.17(9)$ Å $\alpha = \beta = \gamma$=90 deg; $B2/m$ symmetry, extinction coefficient = 0.48(5), twin fraction = 0.121(2); R = 7.66%, wR2 = 16.15%, GooF = 1.39.

La	4*i*	0	−0.00457(4)	0.36096(2)	0.00127(5)	0.4685
Sr	4*i*	0	−0.00457(4)	0.36096(2)	0.00127(5)	0.03125
La	4*i*	0	0.49576(4)	0.13903(2)	0.00129(5)	0.4685
Sr	4*i*	0	0.49576(4)	0.13903(2)	0.00129(5)	0.03125
Cu	2*a*	0	0	0	0.00184(7)	0.25250
Cu	2*d*	1/2	1/2	0	0.00185(7)	0.25250
O	8*j*	0.24995(12)	0.25002(16)	−0.00433(7)	0.00426(17)	1.0
O	4*i*	0	0.0215(6)	0.1806(2)	0.0071(3)	0.5
O	2*i*	0	0.5202(6)	0.3196(2)	0.0078(4)	0.5

TABLE V. Top: Positional and thermal parameters of $La_{1.88}Sr_{0.12}CuO_4$ as obtained from the structure refinement of the neutron (top) and x-ray (bottom) diffraction data sets using the orthorhombic *Bmab* setting.

$La_{1.88}Sr_{0.12}CuO_4$ at 2 K, neutron diffraction $\lambda = 0.794$ Å: $a = 5.34(4)$ Å $b = 5.37(7)$ Å $c = 13.22(0)$ Å $\alpha = \beta = \gamma = 90$ deg; extinction coefficient = 0.037(6), twin fraction = 0.204(4); R = 5.80%, wR2 = 17.05%, GooF = 1.1.

Atom	site	x	y	z	U_{11}	U_{22}	U_{33}	U_{23}	U_{13}	U_{12}	U_{eq}	Occ.
La	8*f*	0	−0.00610(11)	0.36074(5)	0.0013(4)	0.0009(3)	0.0015(3)	0.00007(13)	0	0	0.00121(19)	0.875
Sr	8*f*	0	−0.00610(11)	0.36074(5)	0.0013(4)	0.0009(3)	0.0015(3)	0.00007(13)	0	0	0.00121(19)	0.125
Cu	4*a*	0	0	0	0.0031(6)	0.0023(5)	0.0023(4)	0.00023(18)	0	0	0.0026(2)	1.00
O1	8*e*	1/4	1/4	−0.00583(7)	0.0028(5)	0.0030(4)	0.0045(3)	0	0	−0.0009(3)	0.0034(2)	1.00
O2	8*f*	0	0.0282(3)	0.18252(8)	0.0083(5)	0.0068(4)	0.0022(4)	0.0001(3)	0	0	0.0057(2)	1.00

$La_{1.88}Sr_{0.12}CuO_4$ at 30 K, XRD $\lambda = 0.122$ Å: $a = 5.31(9)$ Å $b = 5.33(9)$ Å $c = 13.17(9)$ Å $\alpha = \beta = \gamma = 90$ deg; extinction coefficient = 0.48(5), twin fraction = 0.121(2); R = 3.63%, wR2 = 13.26%, GooF = 1.17.

La	8*f*	0	−0.00502(2)	0.36094(2)	0.00188(5)	0.00243(6)	0.00076(5)	0.00005(1)	0	0	0.00169(3)	0.875
Sr	8*f*	0	−0.00502(2)	0.36094(2)	0.00188(5)	0.00243(6)	0.00076(5)	0.00005(1)	0	0	0.00169(3)	0.125
Cu	4*a*	0	0	0	0.0029(2)	0.0019(2)	0.0023(1)	0.00008(3)	0	0	0.00234(5)	1
O1	8*e*	1/4	1/4	−0.00491(7)	0.0031(4)	0.0027(4)	0.0062(3)	0	0	0.0003(2)	0.0040(2)	1
O2	8*f*	0	0.0234(3)	0.18330(13)	0.0096(5)	0.0088(4)	0.0034(3)	−0.0016(3)	0	0	0.0073(2)	1

ma, usually called ortho-*m* structures. In these cases the multiplication of the unit cell in the *ab* plane preserves the *Pmmm* symmetry. The biaxial charge order with ordering vectors $\boldsymbol{q} = (1/3, 0, 1/2)$ and $\boldsymbol{q} = (0, 1/3, 1/2)$ is produced by strain waves that break the bilayer mirror symmetry [7]. The CDW modulated structure has been solved and described [7] using a superstructure with *Pmmm* symmetry. Similarly, in LSCO octahedral tilt modes (and their superposition) induce structural distortions leading to a unit cell multiplication with, however, reduced symmetry. The monoclinic distortion, observed over a wide temperature range [18], is displaying long-range correlations along all principal crystal axes. The charge stripe order is, by contrast, extremely weakly correlated across the CuO_2 layers. The two sets of distortions (charge stripe order and monoclinic) are, therefore, not directly linked. Yet future experiments should address whether the monoclinic distortion interacts with superconductivity. It should be addressed, for example, whether the competition between stripe order and superconductivity is channeled through mutual interaction with the monoclinic distortions. Overall, our structural analysis suggests that the weak monoclinic lattice distortions are a necessary condition for charge stripe order in $La_{2-x}Sr_xCuO_4$.

VI. CONCLUSIONS

In summary, we have carried out a neutron and XRD study to resolve the crystal structure underpinning charge stripe order in the high-temperature superconductor $La_{1.88}Sr_{0.12}CuO_4$. The average orthorhombic *Bmab* structure is symmetry inconsistent with the unidirectional charge order. We therefore analyzed atomic distortions away from the average structure that manifest by weak *Bmab*-forbidden Bragg peaks. We infer monoclinic $P2/m$ in the absence of uniaxial pressure and $B2/m$ when uniaxial pressure along the copper-oxygen bond is applied. The $B2/m$ monoclinic space group is also preserved after coupling with the stripe order CDW distortion mode. We therefore conclude that weak monoclinic lattice distortions are a necessary precondition for the emergence of stripe order in $La_{2-x}Sr_xCuO_4$.

ACKNOWLEDGMENTS

R.F., J.K., Q.W., D.B., and J.C. thank the Swiss National Science Foundation for support. R.F. thanks Hans-Beat Bürgi and Stefano Canossa for useful discussions. N.B.C. thanks the Danish Agency for Science, Technology, and Innovation for funding the instrument center DanScatt and acknowledges support from the Q-MAT ESS Lighthouse initiative. Neutron data were collected at the instrument HEiDi jointly operated by RWTH and JCNS at the MLZ within the JARA cooperation. We acknowledge DESY (Hamburg, Germany), a member of the Helmholtz Association HGF, for the provision of experimental facilities. Parts of this research were carried out at beamline P21.1.

[1] M. J. B. Goodenough, G. Demazeau, M. Pouchard, and P. Hagenmuller, J. Solid State Chem. **8**, 325 (1973).
[2] R. J. Cava, A. Santoro, D. W. Johnson, and W. W. Rhodes, Phys. Rev. B **35**, 6716 (1987).
[3] M. F. Garbauskas, R. H. Arendt, and J. S. Kasper, Inorg. Chem. **26**, 3191 (1987).
[4] Q. W. Yan, P. L. Zhang, Z. G. Shen, J. K. Zhao, Y. Ren, Y. N. Wei, T. D. Mao, C. X. Liu, T. S. Ning, K. Sun, and Q. S. Yang, Phys. Rev. B **36**, 8810 (1987).
[5] H. Müller-Buschbaum and A. Teichert, J. Less-Common Met. **155**, 9 (1989).
[6] P. G. Radaelli, D. G. Hinks, A. W. Mitchell, B. A. Hunter, J. L. Wagner, B. Dabrowski, K. G. Vandervoort, H. K. Viswanathan, and J. D. Jorgensen, Phys. Rev. B **49**, 4163 (1994).
[7] E. M. Forgan, E. Blackburn, A. T. Holmes, A. K. R. Briffa, J. Chang, L. Bouchenoire, S. D. Brown, R. Liang, D. Bonn, W. N. Hardy, N. B. Christensen, M. V. Zimmermann, M. Hücker, and S. M. Hayden, Nat. Commun. **6**, 10064 (2015).
[8] G. Grissonnanche, A. Legros, S. Badoux, E. Lefrançois, V. Zatko, M. Lizaire, F. Laliberté, A. Gourgout, J. S. Zhou, S. Pyon, T. Takayama, H. Takagi, S. Ono, N. Doiron-Leyraud, and L. Taillefer, Nature (London) **571**, 376 (2019).
[9] M.-E. Boulanger, G. Grissonnanche, S. Badoux, A. Allaire, É. Lefrançois, A. Legros, A. Gourgout, M. Dion, C. H. Wang, X. H. Chen, R. Liang, W. N. Hardy, D. A. Bonn, and L. Taillefer, Nat. Commun. **11**, 5325 (2020).
[10] G. Grissonnanche, S. Thériault, A. Gourgout, M. E. Boulanger, E. Lefrançois, A. Ataei, F. Laliberté, M. Dion, J. S. Zhou, S. Pyon, T. Takayama, H. Takagi, N. Doiron-Leyraud, and L. Taillefer, Nat. Phys. **16**, 1108 (2020).
[11] M. Braden, G. Heger, P. Schweiss, Z. Fisk, K. Gamayunov, I. Tanaka, and H. Kojima, Physica C Supercond. **191**, 455 (1992).
[12] International Union of Crystallography, Space-group symmetry, in *International Tables for Crystallography*, Vol. A, edited by H. Theo (Springer, Dordrecht, Netherlands, 2005).
[13] Y. Horibe, Y. Inoue, and K. Koyama, Physica C: Superconductivity **282-287**, 1071 (1997), Proceedings of the International Conference on Materials and Mechanisms of Superconductivity High Temperature Superconductors V Part II.
[14] Y. Horibe, Y. Inoue, and Y. Koyama, Phys. Rev. B **61**, 11922 (2000).
[15] N. B. Christensen, J. Chang, J. Larsen, M. Fujita, M. Oda, M. Ido, N. Momono, E. M. Forgan, A. T. Holmes, J. Mesot, M. Huecker, and M. v. Zimmermann, Bulk charge stripe order competing with superconductivity in $La_{2-x}Sr_xCuO_4$ (x=0.12), arXiv:1404.3192 [cond-mat.supr-con].
[16] H. Jacobsen, I. A. Zaliznyak, A. T. Savici, B. L. Winn, S. Chang, M. Hücker, G. D. Gu, and J. M. Tranquada, Phys. Rev. B **92**, 174525 (2015).
[17] M. Reehuis, C. Ulrich, K. Prokeš, A. Gozar, G. Blumberg, S. Komiya, Y. Ando, P. Pattison, and B. Keimer, Phys. Rev. B **73**, 144513 (2006).
[18] A. Singh, J. Schefer, R. Sura, K. Conder, R. F. Sibille, M. Ceretti, M. Frontzek, and W. Paulus, J. Appl. Phys. **119**, 123902 (2016).
[19] A. Sapkota, T. C. Sterling, P. M. Lozano, Y. Li, H. Cao, V. O. Garlea, D. Reznik, Q. Li, I. A. Zaliznyak, G. D. Gu, and J. M. Tranquada, Phys. Rev. B **104**, 014304 (2021).
[20] T. P. Croft, C. Lester, M. S. Senn, A. Bombardi, and S. M. Hayden, Phys. Rev. B **89**, 224513 (2014).

[21] J. C. Toledano and P. Toledano, *The Landau Theory of Phase Transitions* (World Scientific, Singapore, 1987).
[22] P. Tolédano, EPJ Web Conf., **22**, 0007 (2012).
[23] D. M. Hatch and H. T. Stokes, Phys. Rev. B **65**, 014113 (2001).
[24] The $[1,0,0]_{\mathrm{t}}$ and $[0,1,0]_{\mathrm{t}}$ directions are given by $[1,1,0]_{\mathrm{ort}}$ and $[1,\bar{1},0]_{\mathrm{ort}}$ in orthorhombic notation of space group *Bmab*.
[25] S. C. Moss, K. Forster, J. D. Axe, H. You, D. Hohlwein, D. E. Cox, P. H. Hor, R. L. Meng, and C. W. Chu, Phys. Rev. B **35**, 7195 (1987).
[26] T. Kajitani, T. Onozuka, Y. Yamaguchi, M. Hirabayashi, and Y. Syono, Jpn. J. Appl. Phys. **26**, L1877 (1987).
[27] T. Nakano, N. Momono, M. Oda, and M. Ido, J. Phys. Soc. Jpn. **67**, 2622 (1998).
[28] J. Chang, C. Niedermayer, R. Gilardi, N. B. Christensen, H. M. Rønnow, D. F. McMorrow, M. Ay, J. Stahn, O. Sobolev, A. Hiess, S. Pailhes, C. Baines, N. Momono, M. Oda, M. Ido, and J. Mesot, Phys. Rev. B **78**, 104525 (2008).
[29] J. Choi, Q. Wang, S. Jöhr, N. B. Christensen, J. Küspert, D. Bucher, D. Biscette, M. Hücker, T. Kurosawa, N. Momono, M. Oda, O. Ivashko, M. v. Zimmermann, M. Janoschek, and J. Chang, Disentangling intertwined quantum states in a prototypical cuprate superconductor, arXiv:2009.06967 [cond-mat.str-el].
[30] W. Kabsch, Acta Crystallogr., Sect. D **66**, 125 (2010).
[31] G. M. Sheldrick, Acta Crystallogr. A Found Crystallogr. **64**, 112 (2008).
[32] J. Rodríguez-Carvajal, Phys. B: Condens. Matter **192**, 55 (1993).
[33] Here orthorhombic twins imply an interchange of h and k indices.
[34] In the limit of small displacements we aim to produce negligible interference effects with the average structure. This is justified given the observed ratio between the I_{ave} and I_{d} components.
[35] L. D. Landau and E. M. Lifshitz, *Statistical Physics* (Pergamon Press, New York, 1969).
[36] J. M. Perez-Mato, D. Orobengoa, and M. I. Aroyo, Acta Crystallogr., Sect. A **66**, 558 (2010).
[37] In this approach the irreps are fixed by symmetry, and the only free parameters are the amplitudes of the different modes, which can be refined in a standard least-squares fit while keeping fixed the other parameters. It is, thus, possible to determine which of the distortion modes contribute the most to the deviations from a parent average structure. Under the assumption of the harmonic approximation, the distortion modes have a direct correspondence to the phonon eigenvectors.
[38] S. C. Miller and W. F. Love, *Tables of Irreducible Representations of Space Groups and co-representations of magnetic space groups* (Pruett Press, Boulder, Colorado, 1967).
[39] K. S. Aleksandrov, B. V. Beznosikov, and S. V. Misyul, Phys. Stat. Sol. (a) **104**, 529 (1987).
[40] D. M. Hatch, H. T. Stokes, K. S. Aleksandrov, and S. V. Misyul, Phys. Rev. B **39**, 9282 (1989).
[41] B. J. Campbell, H. T. Stokes, D. E. Tanner, and D. M. Hatch, J. Appl. Crystallogr. **39**, 607 (2006).
[42] J. M. Tranquada, B. J. Sternlieb, J. D. Axe, Y. Nakamura, and S. Uchida, Nature (London) **375**, 561 (1995).
[43] G. Ghiringhelli, M. L. Tacon, M. Minola, S. Blanco-Canosa, C. Mazzoli, N. B. Brookes, G. M. D. Luca, A. Frano, D. G. Hawthorn, F. He, T. Loew, M. M. Sala, D. C. Peets, M. Salluzzo, E. Schierle, R. Sutarto, G. A. Sawatzky, E. Weschke, B. Keimer, and L. Braicovich, Science **337**, 821 (2012).
[44] J. Chang, E. Blackburn, A. T. Holmes, N. B. Christensen, J. Larsen, J. Mesot, R. Liang, D. A. Bonn, W. N. Hardy, A. Watenphul, M. v. Zimmermann, E. M. Forgan, and S. M. Hayden, Nat. Phys. **8**, 871 (2012).
[45] A. J. Achkar, R. Sutarto, X. Mao, F. He, A. Frano, S. Blanco-Canosa, M. Le Tacon, G. Ghiringhelli, L. Braicovich, M. Minola, M. Moretti Sala, C. Mazzoli, R. Liang, D. A. Bonn, W. N. Hardy, B. Keimer, G. A. Sawatzky, and D. G. Hawthorn, Phys. Rev. Lett. **109**, 167001 (2012).
[46] M. v. Zimmermann, J. R. Schneider, T. Frello, N. H. Andersen, J. Madsen, M. Käll, H. F. Poulsen, R. Liang, P. Dosanjh, and W. N. Hardy, Phys. Rev. B **68**, 104515 (2003).

Correction: A typographical error in a formula appearing several times throughout the paper has been corrected.